Christoph Nick, Michael Goldhammer, Robert Bestel, Frederik Steger, Andreas W. Daus & Christiane Thielemann

DrCell – A Software Tool for the Analysis of Cell Signals Recorded with Extracellular Microelectrodes

Christoph Nick   *Christoph.nick@h-ab.de*
Department of Engineering, biomems lab
University of Applied Sciences Aschaffenburg,
63743 Aschaffenburg, Germany

Michael Goldhammer   *Michael.goldhammer@h-ab.de*
Department of Engineering, biomems lab
University of Applied Sciences Aschaffenburg,
63743 Aschaffenburg, Germany

Robert Bestel   *Robert.bestel@h-ab.de*
Department of Engineering, biomems lab
University of Applied Sciences Aschaffenburg,
63743 Aschaffenburg, Germany

Frederik Steger   *Frederik.steger@hotmail.de*
Department of Engineering, biomems lab
University of Applied Sciences Aschaffenburg,
63743 Aschaffenburg, Germany

Andreas W. Daus   *Andreas.daus@h-ab.de*
Department of Engineering, biomems lab
University of Applied Sciences Aschaffenburg,
63743 Aschaffenburg, Germany

Christiane Thielemann   *christiane.thielemann@hotmail.de*
Department of Engineering, biomems lab
University of Applied Sciences Aschaffenburg,
63743 Aschaffenburg, Germany

Abstract

Microelectrode arrays (MEAs) have been applied for in vivo and in vitro recording and stimulation of electrogenic cells, namely neurons and cardiac myocytes, for almost four decades. Extracellular recordings using the MEA technique inflict minimum adverse effects on cells and enable long term applications such as implants in brain or heart tissue.

Hence, MEAs pose a powerful tool for studying the processes of learning and memory, investigating the pharmacological impacts of drugs and the fundamentals of the basic electrical interface between novel electrode materials and biological tissue. Yet in order to study the areas mentioned above, powerful signal processing and data analysis tools are necessary.

In this paper a novel toolbox for the offline analysis of cell signals is presented that allows a variety of parameters to be detected and analyzed. We developed an intuitive graphical user interface (GUI) that enables users to perform high quality data analysis. The presented MATLAB® based toolbox gives the opportunity to examine a multitude of parameters, such as spike and neural burst timestamps, network bursts, as well as heart beat frequency and signal propagation for cardiomyocytes, signal-to-noise ratio and many more. Additionally a spike-sorting tool is included, offering a powerful tool for cases of multiple cell recordings on a single microelectrode.

Christoph Nick, Michael Goldhammer, Robert Bestel, Frederik Steger, Andreas W. Daus & Christiane Thielemann

For stimulation purposes, artifacts caused by the stimulation signal can be removed from the recording, allowing the detection of field potentials as early as 5 ms after the stimulation.

Keywords: MATLAB® Toolbox, Bio Signal Processing, Spike Sorting, Network Analysis, Extracellular Recording.

---

1. INTRODUCTION

For all neural or cardiac implants, cell activity is detected by extracellular electrodes in the form of field potentials. Since cortical implants might be used someday to control artificial limbs, wheelchairs or software [1, 2], improving the living conditions of disabled people, the field of neural signal processing is of utmost importance.

Yet signal processing is not only essential for in vivo applications such as implants, but also for in vitro studies of neural as well as cardiac networks that require substantial amounts of data processing. These systems are a powerful tool for studying learning, memory [3] and pharmacologic mechanisms [4]. In addition, the properties of the interface between novel electrode materials and biological tissue can be investigated [5], especially as there has been a growing community utilizing different kinds of multi-electrode arrays for in vivo and in vitro experiments in the recent past. Although the MEAs being used may differ in electrode size, substrate and electrode material as well as in number of electrodes, they all share the same working principles: (1) extracellular microelectrodes do not penetrate the cell membrane. (2) They record field potentials in the vicinity of the cell caused by changes in membrane potential – so called action potentials (AP). (3) The cells are either cultured onto the electrode array for in vitro studies or the chip is implanted into living tissue for in vivo studies. (4) These electrodes can be used to stimulate cells through voltage or current pulses.

There are a couple of software toolboxes for neuronal signal processing available, where only a few are specifically designed for extracellular signals recorded by microelectrode arrays. These toolboxes include the commercially available MC_Rack (multichannel systems, Reutlingen, Germany), NeuroExplorer (Nex Technologies, Littleton, MA, USA), Offline Sorter (Plexon, Dallas, TX, USA) or NeuroMAX (R.C. Electronics Inc, Santa Barbara, CA, USA) and, furthermore, the open source projects FIND [6] sigTool [7] or nStat [8] to name only a few. Most of these toolboxes focus on neural signal processing exclusively, whereas cardio tools have not received as much attention. This motivated us to develop an open toolbox including established as well as new algorithms like a novel spike sorting algorithm that enable analysis of a variety of parameters for neural and cardiac cell signals.

In the following we introduce an offline signal processing toolbox with algorithms for spike and burst detection, a sophisticated algorithm for spike sorting, spike overlay and signal propagation for cardiac cells and furthermore an analysis of simultaneous neural network activity.

There are several cells that can change their resting potential e.g. neurons and cardiac myocytes. Throughout this paper we use the term spike to describe such a voltage peak no matter which cell caused it. Since the software tool reported herein is capable of working with any kind of spike we do not distinguish between different kinds of cell signals.

This multi domain approach combined with powerful tools for neural and cardiac signals is unique in the field of offline analysis of electrophysiological data.

The GUI, provides researchers an easy to use platform to process their signals and test new, custom made algorithms. A flow chart of available processing steps is shown in Figure 1. Generally the algorithms are designed for microelectrode arrays with 60 electrodes, yet signals originating from other set ups such as needle arrays or arrays with a different number of working electrodes can be processed as well.

Christoph Nick, Michael Goldhammer, Robert Bestel, Frederik Steger, Andreas W. Daus & Christiane Thielemann

The software is distributed under the GNU general public license (GPL) version 3 and is available from the authors at www.h-ab.de/drcell. It is based on MATLAB® R2012a including the Curve Fitting, Image Processing, Signal Processing, Statistics and Wavelet toolboxes.
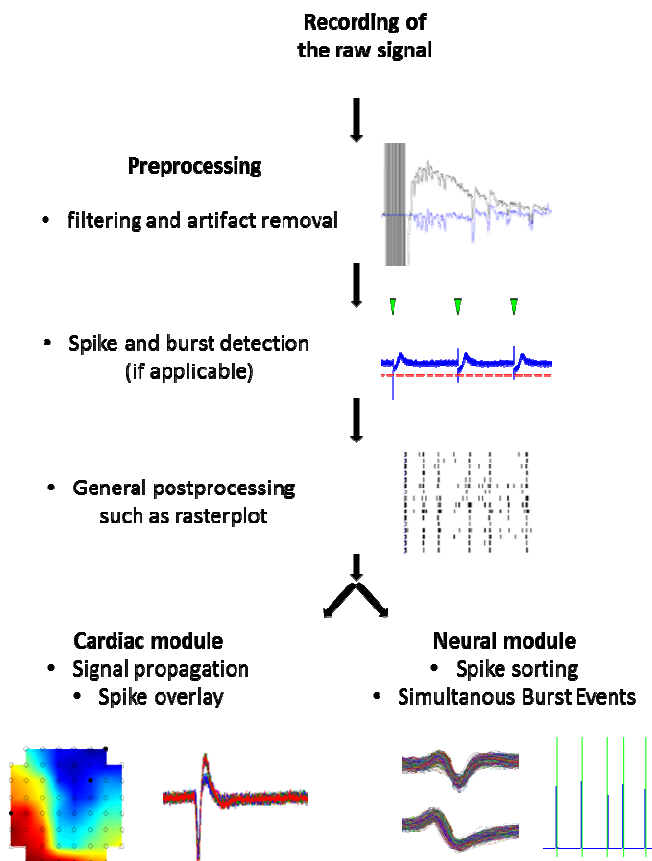

FIGURE 1: Flow chart of possible processing steps in the "DrCell" software toolbox.

To test the developed algorithms cell culture experiments were conducted. Data recording was done using a multichannel system amplifier stage combined with custom made LabVIEW [TM] based software. Details about cardiac cell cultures can be found in [5] Details about neural cell cultures in [9]. In short, cortical rat neurons were purchased cry conserved from Lonza Ltd (Lonza Ltd, Basel, Switzerland). Before cultivation, microelectrode arrays were coated with Poly-D-Lysine (PDL, 0,1 mg/ml in phosphate buffered saline (PBS), Sigma-Aldrich Chemie GmbH, Taufkirchen, Germany) and Laminin (15 µg/ml in PBS, Sigma-Aldrich Chemie GmbH). Spikes were recorded from day 14 in vitro.

Cardiac myocytes were prepared from chick embryos (E8). Hearts were carefully removed, the tissue dissociated and the cells cultured onto the MEAs. Here the chips were coated with Fibronectin (10 µg/ml in PBS,Sigma-Aldrich Chemie GmbH) prior to cultivation.

2. RESULTS AND DISCUSSION
The software tool named "DrCell" is subdivided into general preprocessing tools and a specific module for cardiomyocytes as well as a module designed for neural signal processing and analysis. While the cardiac module includes algorithms to analyze the contraction rate of the

Christoph Nick, Michael Goldhammer, Robert Bestel, Frederik Steger, Andreas W. Daus & Christiane Thielemann

tissue and signal propagation across the electrode array, the neural module features algorithms developed to analyze bursts and network behavior.

2.1 Preprocessing

In order to enable or just improve the detectability of signal parameters, it is advantageous to apply preprocessing algorithms to the recorded data. This includes digital filtering, spike detection and spike sorting for neuronal signals as well as the removal of stimulation artifacts in the case of an electrical stimulation.

The graphical user interface of the MATLAB® software tool allows loading of ASCII files, containing recorded data, into the workspace for further processing. If the data is not recorded in ASCII file format it must first be converted using freely available tools such as the MC_DataTool from multichannel systems.

In a first step the signal can be filtered by a bandstop or a bandpass filter. The frequencies for the lower and upper stopband edge frequencies can be set manually by the user. If both values are identical a notch filter with 1 dB passband ripple is applied at the chosen frequency. For the bandfilter an IIR Chebyshev filter with 20 dB stop band attenuation and ripple in the stopband is used.

In addition, noisy electrodes can be omitted completely and stimulation artifacts can be removed as described in detail later. The next processing steps include the calculation of thresholds, spike and burst detection as well as several post processing tools such as spike sorting, analysis of network bursts, correlation analysis and spike shape analysis.

2.2 Spike Detection

The overall quality of the data analysis depends on the reliability of spike detection. Only if spikes are detected correctly, bursts, simultaneous bursts (bursts that appear over multiple electrodes at the same time), interspike intervals, or shapes of spikes can be detected and analyzed correctly. Out of a broad variety of spike detection methods, the first reported and still widely applied algorithm uses a negative multiple of the root mean square (rms), or alternately of the standard deviation of the base noise, as threshold. If the signal voltage drops below this value, a spike is detected [10]. Variations of this very easy, fast and reliable algorithm are also available e.g. multiple thresholds [11] or in combination with additional pattern recognition algorithms [12].

The spike detection algorithm implemented in DrCell works in four steps, which are summarized here and explained in detail below: (1) A time frame of two seconds on each electrode containing exclusively noise is detected. (2) For this frame the root mean square (rms) value and the standard deviation are calculated and (3) multiplied with a negative factor. As default value a multiple of the rms is used as threshold; alternatively a multiple of the standard deviation can be chosen instead. (4) The absolute minimum of every voltage peak that is lower than the threshold is saved as the spike's timestamp.

(1) To detect the base noise level, a time window is shifted over the signal of each channel searching for spike-free periods. The size of the window is set to 50 ms as default value but can be adjusted by the user. The detection of spike free windows is achieved by fitting the signal histogram with a Gaussian distribution, typical for white noise. A low standard deviation (equal or lower than a value defined by the user and set as default to ≤ 5) from this Gaussian distribution is interpreted as pure, spike-free noise. In this case the noise data is saved in a separate array and the window is shifted forward by one window length. If the standard deviation is higher than the defined value spikes are likely to be present in that particular interval and the window is only shifted half the window length and conditions are checked again. This process is repeated until a time period of 2 seconds is identified as "spike-free". Sometimes the signal-to-noise ratio is too low for any signal to be detected. If half of the total recording time has been swept and no spike-free window has been found, the algorithm stops and this particular electrode is labeled "noisy", hence being disregarded for any further analysis.

As an option, the user can also define the timeframe to be used for calculating the rms value or standard deviation of the noise manually.

(2-3) The rms value or, respectively, the standard deviation of these spike free signal arrays is multiplied by an empiric factor of -6 (default value) to set the threshold. This factor can also be set manually in the range of -3 to -14.

In addition, a refractory time between spikes can be defined, if whished by the user. In this case the algorithm works as defined above but, after saving all timestamps, the intervals between the spikes are checked for physiological plausibility and, if this is not given, the second spike is erased from the array.

The signal-to-noise ratio (SNR) of biological signals is not easily determined. In general the SNR is defined as the signal-power divided by the noise-power. Since only field potentials are measured, in other words voltage signals, there is no information on the respective power. Therefore we define the SNR of each electrode as SNR = $(v_{ps}/\sigma_n)^2$, while vps describes the average peak voltage of spikes and σn the standard deviation of the noise [5]. By assuming the same impedance for signal and noise amplitudes the power ratio is calculated by squaring the fractal expression.

This algorithm provides a very reliable and fast method for spike detection and is also easily implementable for online analysis.

2.3   Stimulation Artifact Removal
If cells are stimulated by electrical impulses supplied by a current or a voltage source [3], cell responses may be superimposed by undesirable distortions. Here we distinguish between crosstalk originating from the stimulation signal itself (about -18 ms to 0 ms in Fig. 3) and artifacts that appear shortly after the stimulation (about 0 ms until 80 ms in Fig. 3). Typically, cell reactions to the stimulation are expected within the first few milliseconds after the end of stimulation, while artifacts last up to 100 ms; therefore the removal of artifacts is desirable [13]. There are several approaches to achieve cancellation of artifacts described in the literature: the separation of stimulation and recording electrodes [14], the application of sample and hold elements [15], pass filters [16] or algorithms to restore the disturbed signal [13, 17].

The algorithm implemented in the DrCell toolbox reduces the critical time after a stimulus from about 100 ms to below 10 ms. For this purpose the beginning and end of the stimulation period is detected by a threshold based algorithm. The artifact signal is fitted by two consecutive 9th order polynomials, one for the period between 0.5 and 7.5 ms and one for 7.5 to 82.5 ms after stimulation. Subtraction of these polynomials from the recorded signal reduces distortions significantly (see Figure 2). In case the first couple of milliseconds (1 - 5 ms) are severely distorted, this time interval may be completely removed (set to 0 V), just as the stimulation interference itself.
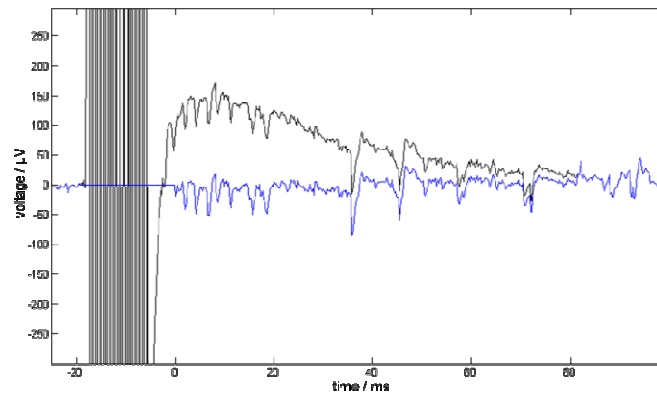
FIGURE 2: Effect of artifact removal. Stimulation crosstalk (-18 ms to 0 ms) and artifacts (about 0 ms until 80 ms) are removed from the distorted original signal (black) resulting in an adjusted signal (blue). This step clearly facilitates the spike detection immediately after stimulation.

According to Ruaro [16] applying ninth order polynomials will result in robust artifact removal, while higher order polynomials would unnecessarily increase the computation cost. The application of polynomials of lesser order can still result in corrupted artifact removal.

Cardiac Module
2.4   Beat Rate
Regular and synchronous contraction is a key feature of cardiac tissue. Pacemaker cells have the ability to initiate action potentials that propagate via gap junctions within a functional syncytium. In cardiac myocytes cultured on MEAs, the contraction rate correlates over time with the intrinsic field potentials and thus can be analyzed in terms of beat rate or for possible arrhythmias [18]. In our experiments, the former is calculated by the reciprocal median of the Interspike intervals (ISIs). The regularity is estimated using the median absolute deviation (MAD) of reciprocal ISIs [19].

2.5   Spike Shape and Propagation
Typically the course of field potentials can be divided into several phases identified by negative or positive peaks, respectively. Applying chemical or electrical stimuli to the cells, as well as the effects of aging may influence several characteristics of the spike shape, e.g. the general field action potential duration, amplitude or the repolarization time. Therefore some domains might be prolonged or reduced and might occur either delayed or prematurely, respectively, whereas some characteristics of spike shape may become less distinctive or may even disappear.

In cultures of cardiac tissue, the signal generated by pacemaker cells spreads throughout the whole network. As a consequence it is interesting to investigate the origin, direction and propagation speed of the specific signal. For this purpose an algorithm is implemented that maps almost synchronous spikes in a false color map by applying a time scale in the two dimensions of the electrode array (Figure 3 top). Noisy electrodes without discernible spikes or electrodes manually omitted from the analysis are highlighted in black. To further facilitate propagation pathway identification, arrows may be superimposed indicating propagation direction and speed (length of the arrows), not shown.
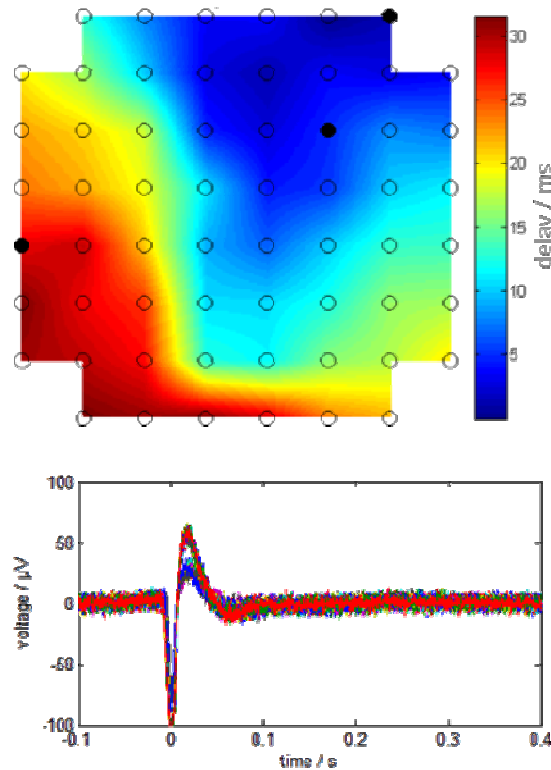
Christoph Nick, Michael Goldhammer, Robert Bestel, Frederik Steger, Andreas W. Daus & Christiane Thielemann

FIGURE 3: Propagation and spike overlay. The propagation of one heartbeat over the electrode array is shown (top). A spike overlay is displayed, where two different spike forms can clearly be distinguished (bottom).

The propagation algorithm is based on the detection of the first spike appearing on the MEA. Delayed spikes within the next 200 ms are identified and their retard and electrode position are used to calculate speed and propagation pathways which are visualized on a virtual MEA layout.

To address the issue of varying spike shapes, the DrCell algorithm determines characteristic peaks of each spike and the interval between these peaks. In addition, these data are not only calculated for just one spike, but may either be assessed for all spikes recorded by a single electrode or as mean values of the spikes recorded by all electrodes, further including information about their standard deviation and median. A graphic panel depicts an overlay of all spikes recorded on a single electrode (Figure 3 bottom), allowing an easy assessment of continued conformity of the spike shapes. The algorithm uses detected spikes and displays a time frame [spike time - x; spike time + y] of each selected spike.

This panel proves especially valuable when working with cardiac tissues, as comparison of the duration of the field action potentials presents a valid method to evaluate the risk of diverse heart diseases. Of course, observation of single spikes is an option as well. In this case, the user may switch from one recorded spike to the next receiving single spike data, also allowing manual query of time points during the measurement.

With these tools at hand the electrophysiological effects of aging, electrical or pharmacologic stimuli can be easily detected and tracked throughout the course of experiment.

Neural Module
2.6 Spike Sorting
With a typical electrode diameter of 20 - 30 μm, each electrode is capable of recording signals from several cells at once. Especially for neural cell cultures it is crucial to identify the network activity on a single cell level, as subsequent analysis, such as burst or network burst detection, is

primarily based on this information. Under the assumption that the coupling between an individual cell and its respective electrode creates a unique spike shape characteristic, several pattern-matching methods, called spike-sorting algorithms, have been developed in order to address this task. The DrCell framework provides a unique spike-sorting algorithm for this purpose, which is described in detail in [20].

Unlike other spike sorting algorithms that exclusively use a specific type of feature, such as principal components [21, 22] or certain Wavelet based coefficients [23], the implemented algorithm calculates a variety of features and chooses the most suitable in a subsequent step. In order to distinguish the features most suitable for discriminating the spike shapes present in the recorded signal, the probability distribution of each derived feature is calculated over all detected spikes. The distributions are then evaluated with the expectation maximization algorithm (EM) that approximates the derived probability functions with a mixture of Gaussians. This allows an identification of multimodal distributed features that have the potential of discriminating different spike shapes. The features with the most distinguishable multimodal character are chosen for the final clustering step, with the correlation between the particular features serving as an additional criterion. In the last step the spikes are clustered into distinct groups on the basis of the determined set of features. Many sorting algorithms differ not only in the chosen set of features but also in their classification methods, and either use simple clustering, e.g. k-means [20], fuzzy c-means [22] or superparamagnetic clustering [23] or favor more complex classification algorithms using artificial neural networks [24] or support vector machines [25]. Since the latter classification algorithms usually require extensive and difficult training with specifically designed data, an expectation maximization clustering method was chosen in this context, as this approach fits best into the overall spike sorting algorithm. As shown in Figure 4, the described spike sorting process allows the discrimination of different spike shapes, in other words different cell signals, from each other.
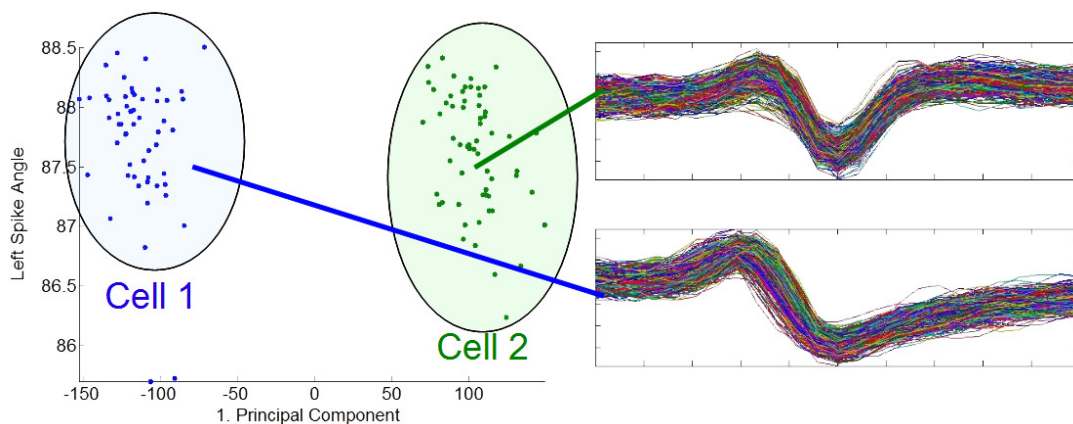

FIGURE 4: Sorting result for two spiking neurons recorded by one electrode. Two different spike shapes can clearly be distinguished.

Thus, the results of any following analysis of network activity or network information processing can be significantly enhanced and more detailed interpretation is possible.

2.7 Burst Detection

The definition of a burst varies in the literature, but most sources use already detected spikes to find possible burst events. Since there is no commonly accepted definition, we describe some definitions from the literature and then explain the implemented algorithms in detail. It should be mentioned that each definition has consequences with regard to the number and time of detected bursts and thus may alter the results.

Christoph Nick, Michael Goldhammer, Robert Bestel, Frederik Steger, Andreas W. Daus & Christiane Thielemann

One of the oldest methods to detect a burst is based on purely statistical means. A burst is found in this case by analyzing the interspike intervals (ISIs). An unexpected series of short ISIs is then defined as a burst [26].

In contrast to this approach, there are several definitions stating that a burst consists of a certain number of spikes within a specific timeframe. Turnbull defines a burst as a series of 2–5 spikes with a maximum interspike interval of 12-50 ms, with the exact value of these parameters being adjustable according to individual needs [27]. Chagnac-Amital defines a burst as a series of at least three spikes, with no interspike interval being set [28]. Martinoia and Chiappalone both define a burst as a series of at least 10 spikes, with the interval between two spikes not exceeding 100 ms [10, 29]. Corner defines several kinds of bursts. A mini-burst is a series of at least three spikes with a maximum interspike interval of 100 ms, with only the spikes of a specific electrode being considered. A midi-burst is a series of at least three spikes with a maximum interspike interval of 1000 ms on more than one electrode [30]. Baker adds another burst-species – a micro burst. This kind of burst is a series of at least three spikes with a maximum interspike interval of 10 ms [31].
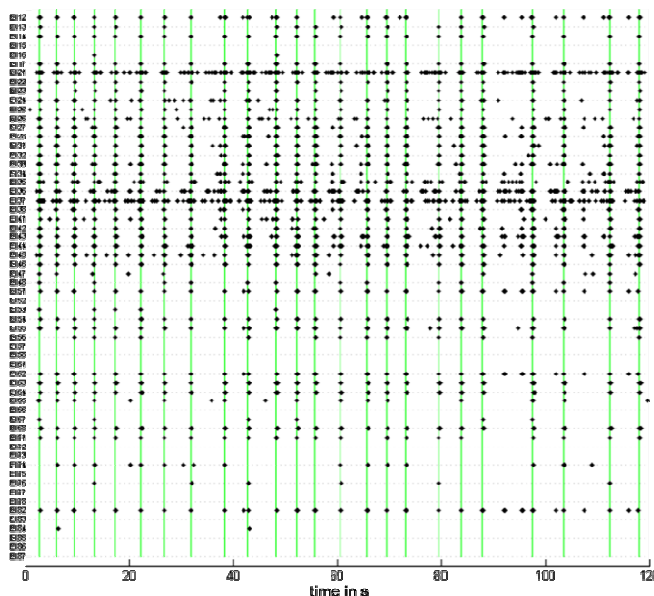

FIGURE 5: Raster plot of all recorded electrodes. Each spike is represented by one dot. Simultaneous burst events are marked by a green line.

According to Wagenaar, a burst is a group of spikes with a certain interspike interval [32]. The limit for the interspike interval is either 100 ms or (4 times the average spike rate (spikes/second))-1, whichever is less. After four spikes with these parameters are found, the interspike interval is set to the minimum of (3 times the average spike rate)-1 and 200 ms and more spikes that meet these criteria are searched before and after this core group.

Jungblut defines a burst based on definitions by [10, 32] as a series of at least 3 spikes with the interspike interval of the first two spikes not exceeding 10 ms and with the ISI of the following spikes no longer than 20 ms [34].

Several of the algorithms mentioned above are implemented in the DrCell software. As default parameters we set a definition that is equivalent to Jungblut´s burst. The settings can be manually changed so that other definitions of bursts can also be used, e.g. the algorithm for Corner´s mini-burst or the definition of Wagenaar with at least 3 or 4 spikes per burst. For analyzing cardiac cells there is no burst and the ISI interval can be set to either 100 ms or 200 ms. All definitions are only default values and can be adjusted as the operator wishes.

The first spike of the burst is taken as the burst timestamp and the time difference between the first and last spike is saved as the burst duration. The interburst interval is calculated between the last spike of the nth burst and the first spike of the (n+1)th burst. These values are calculated and saved as averages with standard deviation for each channel and for all channels. Furthermore, the average number of spikes per burst is saved for each electrode as well as for the whole electrode array. The detected spikes and bursts are marked in the signal and can be viewed additionally as a spike train or as a raster plot (Figure 5).

2.8 Network Behavior
The occurrence of simultaneous burst events (SBEs) as shown in Figure 6 can be seen as an indicator of the connections and communication within the neural network.

A burst is typically generated in a certain area of the network and then spreads across the whole array, which leads to nearly simultaneous bursts at multiple electrodes. Depending on how well a neural network is connected, these synchronous events occur rarely to frequently (1 – 30 per minute) and show different speeds of propagation [35].

Because of the large number of possible connections (each cell on the chip can form up to 10,000 synapses) between the neurons and thus the possible paths the signal can propagate, it is impossible to determine the exact pathway by evaluating the burst timestamps on the various electrodes.

However, by evaluating the direction of signal propagation, it can be determined whether network bursts consistently start from the same region and if they are propagated along similar pathways [36]. Further, the number of electrodes that are involved in a network burst and the time between the first and the last burst (propagation speed) can be evaluated.

Similar to regular bursts, there are different definitions of network bursts. Van Pelt assumes that the number of active electrodes and the spike rate of each electrode are increased if a network burst occurs. Thus, the product of the number of active electrodes and the total spike rate can serve as a detection criterion [37]. Other definitions use the already detected spikes and bursts instead, yet differ in the required number of electrodes that take part in the network event.

In the algorithm by Segev, at least 80% of all active electrodes must show activity within a 100 ms time window [38]. This algorithm proves to be reliable in general although we found that the criterion of at least 80% of all active electrodes being active simultaneously is very strict. Thus in DrCell the number of simultaneous active electrodes is set to five. After a burst has been detected, the algorithm checks for other active electrodes exhibiting a burst-event between 40 ms before and after the initially detected burst. If at least five such electrodes are found, the maximum of the resulting histogram of timestamps is called the network burst.

The histogram is then smoothened by a filter and the timestamps at 20% and 80% of the maximum before and after each network burst are saved. Based on these timestamps the rising time (20% - 80% before peak), the falling time (80% - 20% after peak) and the duration (20% before - 20% after) are calculated and saved. For the entire array all values are given with their minimum, maximum and average value including the standard deviation. Furthermore, the number of the participating electrodes is also stored, making a comparison between experiments straightforward.

Finally, in order to evaluate the similarity between two electrodes, the cross correlation can be calculated. The correlation is quantified by Cohen´s Kappa, with a general value range between 0, meaning no correlation at all, and 1 meaning complete equality [39]. Additionally, the auto correlation can be calculated to evaluate the regularity of spikes or bursts.

Christoph Nick, Michael Goldhammer, Robert Bestel, Frederik Steger, Andreas W. Daus & Christiane Thielemann

3. CONCLUSION AND OUTLOOK

In this paper we present a software toolbox for the analysis of cell signals, regarding both neurons and cardiac cells that are recorded with microelectrode arrays. This toolbox thereby covers not only all basic processing algorithms such as spike detection, but also features a multitude of advanced algorithms for both neural and cardiac signals. It allows, for instance, the investigation of spike propagation behavior and, furthermore, the identification of single or multiple pacemaker centers in cardiomyocyte cultures. When faced with neuronal data, the toolbox provides a wide range of spike and burst analysis methods, such as spike sorting, burst and network burst analysis and even facilitates the handling of datasets recorded in stimulation experiments. Unlike many commercially available tools, the presented framework furthermore enables the user to customize or even add specific methods or features. This allows the user to alter, for example, the display of results according to individual needs or desires. It further permits the user to implement, for instance, new spike or burst criteria or even completely new processing methods in addition to the existing algorithms. New algorithms or functions can be called by prepared empty menu-buttons. Here Matlab, which is available at most research institutions, provides a very powerful environment to develop novel algorithms.

In the near future we will implement parts of this toolbox into our recording system for online analysis of cultured networks. Especially an online spikesorting algorithm will be very helpful for online analysis. We also plan to add more algorithms that will support the user in automatically analyzing sets of data and comparing their results. Further advancement of the algorithms include the propagation of signals over the array or analyzing network behavior by simulating neural networks with known mathematically models.

Furthermore the toolbox will serve as analytical tool for future cell culture tests, where the effects of radiation on the biological tissue are studied. In addition, recently developed Matlab® toolboxes such as the parallel computing toolbox allow various adaptations to Dr. Cell. As the presented software can be changed freely, this toolbox can be used to transform the Dr. Cell software into a GPU environment, processing individual electrodes independently and in parallel, hence speeding up the data analysis significantly.

4. REFERENCES

[1] M. Nicolelis and J. Chapin, "Controlling robots with the mind," Scientific American-American Edition, vol. 287, no. 4, pp. 46–55, 2002.

[2] M. Velliste, S. Perel, M. Spalding, A. Whitford, and A. Schwartz, "Cortical control of a prosthetic arm for self-feeding," Nature, vol. 453, no. 7198, pp. 1098–1101, 2008.

[3] D. Wagenaar, R. Madhavan, J. Pine, and S. Potter, "Controlling bursting in cortical cultures with closed-loop multi-electrode stimulation," Journal of Neuroscience, vol. 25, no. 3, pp. 680–688, 2005.

[4] A. Daus, P. Layer, and C. Thielemann, "A spheroid-based biosensor for the label-free detection of drug-induced field potential alterations," Sensors and Actuators B: Chemical, vol. 165, no. 1, pp. 53–58, 2012.

[5] C. Nick, R. Joshi, J. Schneider, and C. Thielemann, "Three-dimensional carbon nanotube electrodes for extracellular recording of cardiac myocytes." Biointerphases, vol. 7, no. 1-4, pp. 58–64, 2012.

[6] R. Meier, U. Egert, A. Aertsen, and M. Nawrot, "Find - a unified framework for neural data analysis," Neural Networks, vol. 21, no. 8, pp. 1085–1093, 2008.

[7] M. Lidierth et al., "sigtool: A matlab-based environment for sharing laboratory-developed software to analyze biological signals," Journal of neuroscience methods, vol. 178, no. 1, pp. 188–196, 2009.

[8] I. Cajigas, W. Malik, and E. Brown, "nstat: Open-source neural spike train analysis toolbox for matlab," Journal of Neuroscience Methods, vol. 211, no. 2, pp. 245—264, 2012.

[9] C. Nick, S. Quednau, R. Sarwar, H.F. Schlaak and C. Thielemann, "High Aspect Ratio Gold Nanopillars on Microelectrodes for Neural Interfaces", submitted.

[10] M. Chiappalone, A. Novellino, I. Vajda, A. Vato, S. Martinoia, and J. Van Pelt, "Burst detection algorithms for the analysis of spatio-temporal patterns in cortical networks of neurons," Neurocomputing, vol. 65, pp. 653–662, 2005.

[11] T. Borghi, R. Gusmeroli, A. Spinelli, and G. Baranauskas, "A simple method for efficient spike detection in multiunit recordings," Journal of neuroscience methods, vol. 163, no. 1, pp. 176–180, 2007.

[12] P. Thakur, H. Lu, S. Hsiao, and K. Johnson, "Automated optimal detection and classification of neural action potentials in extra-cellular recordings," Journal of Neuroscience Methods, vol. 162, no. 1-2, pp. 364–376, 2007.

[13] D. Wagenaar and S. Potter, "Real-time multi-channel stimulus artifact suppression by local curve fitting," Journal of neuroscience methods, vol. 120, no. 2, pp. 113–120, 2002.

[14] A. Grumet, J. Wyatt, and J. Rizzo, "Multi-electrode stimulation and recording in the isolated retina," Journal of neuroscience methods, vol. 101, no. 1, pp. 31–42, 2000.

[15] Y. Jimbo, H. Robinson, and A. Kawana, "Strengthening of synchronized activity by tetanic stimulation in cortical cultures: application of planar electrode arrays," Biomedical Engineering, IEEE Transactions on, vol. 45, no. 11, pp. 1297–1304, 1998.

[16] Y. Jimbo and A. Kawana, "Electrical stimulation and recording from cultured neurons using a planar electrode array," Bioelectrochemistry and Bioenergetics, vol. 29, no. 2, pp. 193–204, 1992.

[17] M. Ruaro, P. Bonifazi, and V. Torre, "Toward the neurocomputer: Image processing and pattern recognition with neuronal cultures," Biomedical Engineering, IEEE Transactions on, vol. 52, no. 3, pp. 371–383, 2005.

[18] U. Egert and T. Meyer, Heart on a Chip - Extracellular Multielectrode Recordings from Cardiac Myocytes in Vitro. Springer Berlin Heidelberg, 2005, ch. Heart on a Chip - Extracellular Multielectrode Recordings from Cardiac Myocytes in Vitro, pp. 432–453.

[19] A. Daus, M. Goldhammer, P. Layer, and C. Thielemann, "Electromagnetic exposure of scaffold-free three-dimensional cell culture systems." Bioelectromagnetics, vol. 32, no. 5, pp. 351–359, 2011.

[20] R. Bestel, A. Daus, and C. Thielemann, "A novel automated spike sorting algorithm with adaptable feature extraction," Journal of Neuroscience Methods, vol. 211, no. 1, pp. 168–178, 2012.

[21] G. Wang, Y. Zhou, A. Chen, P. Zhang, and P. Liang, "A robust method for spike sorting with automatic overlap decomposition," Biomedical Engineering, IEEE Transactions on, vol. 53, no. 6, pp. 1195–1198, 2006.

[22] J. Choi, H. Jung, and T. Kim, "A new action potential detector using the mteo and its effects on spike sorting systems at low signal-to-noise ratios," Biomedical Engineering, IEEE Transactions on, vol. 53, no. 4, pp. 738–746, 2006.

[23] R. Quiroga, Z. Nadasdy, and Y. Ben-Shaul, "Unsupervised spike detection and sorting with wavelets and superparamagnetic clustering," Neural Computation, vol. 16, pp. 1661–1687, 2004.

[24] P. Horton, A. Nicol, K. Kendrick, and J. Feng, "Spike sorting based upon machine learning algorithms (soma)," Journal of neuroscience methods, vol. 160, no. 1, pp. 52–68, 2007.

[25] R. Vogelstein, K. Murari, P. Thakur, C. Diehl, S. Chakrabartty, and G. Cauwenberghs, "Spike sorting with support vector machines," in Engineering in Medicine and Biology Society, 2004. IEMBS'04. 26th Annual International Conference of the IEEE, vol. 1. IEEE, 2004, pp. 546–549.

[26] C. Legendy and M. Salcman, "Bursts and recurrences of bursts in the spike trains of spontaneously active striate cortex neurons," Journal of neurophysiology, vol. 53, no. 4, pp. 926–939, 1985.

[27] L. Turnbull, E. Dian, and G. Gross, "The string method of burst identification in neuronal spike trains," Journal of neuroscience methods, vol. 145, no. 1-2, pp. 23–35, 2005.

[28] Y. Chagnac-Amitai, H. Luhmann, and D. Prince, "Burst generating and regular spiking layer 5 pyramidal neurons of rat neocortex have different morphological features," The Journal of Comparative Neurology, vol. 296, no. 4, pp. 598–613, 1990.

[29] S. Martinoia, P. Massobrio, M. Bove, and G. Massobrio, "Cultured neurons coupled to microelectrode arrays: circuit models, simulations and experimental data," Biomedical Engineering, IEEE Transactions on, vol. 51, no. 5, pp. 859–863, 2004.

[30] M. Corner, J. Van Pelt, P. Wolters, R. Baker, and R. Nuytinck, "Physiological effects of sustained blockade of excitatory synaptic transmission on spontaneously active developing neuronal networks–an inquiry into the reciprocal linkage between intrinsic biorhythms and neuroplasticity in early ontogeny," Neuroscience & Biobehavioral Reviews, vol. 26, no. 2, pp. 127–185, 2002.

[31] R. Baker, M. Corner, and J. van Pelt, "Spontaneous neuronal discharge patterns in developing organotypic mega-co-cultures of neonatal rat cerebral cortex," Brain research, vol. 1101, no. 1, pp. 29–35, 2006.

[32] D. Wagenaar, T. DeMarse, and S. Potter, "Meabench: A toolset for multi-electrode data acquisition and on-line analysis," in Neural Engineering, 2005. Conference Proceedings. 2nd International IEEE EMBS Conference on. Ieee, 2005, pp. 518–521.

[33] D. Tam, "An alternate burst analysis for detecting intra-burst firings based on inter-burst periods," Neurocomputing, vol. 44, pp. 1155–1159, 2002.

Christoph Nick, Michael Goldhammer, Robert Bestel, Frederik Steger, Andreas W. Daus & Christiane Thielemann

[34] M. Jungblut, W. Knoll, C. Thielemann, and M. Pottek, "Triangular neuronal networks on microelectrode arrays: an approach to improve the properties of low-density networks for extracellular recording," Biomedical Microdevices, vol. 11, no. 6, pp. 1269–1278, 2009.

[35] D. Eytan and S. Marom, "Dynamics and effective topology underlying synchronization in networks of cortical neurons," The Journal of neuroscience, vol. 26, no. 33, pp. 8465–8476, 2006.

[36] J. Rolston, D. Wagenaar, and S. Potter, "Precisely timed spatiotemporal patterns of neural activity in dissociated cortical cultures," Neuroscience, vol. 148, no. 1, pp. 294–303, 2007.

[37] J. van Pelt, P. Wolters, W. Rutten, M. Corner, P. Van Hulten, and G. Ramakers, "Spatio-temporal firing in growing networks cultured on multi-electrode arrays," in World Congress on Neuroinformatics 2001, 2001.

[38] R. Segev, M. Benveniste, E. Hulata, N. Cohen, A. Palevski, E. Kapon, Y. Shapira, and E. Ben-Jacob, "Long term behavior of lithographically prepared in vitro neuronal networks," Physical review letters, vol. 88, no. 11, p. 118102, 2002.

[39] J. Cohen, "Weighted kappa: Nominal scale agreement provision for scaled disagreement or partial credit," Psychological bulletin, vol. 70, no. 4, pp. 213–220, 1968.